

Synthesis and Physicochemical Characterization of a New Gadolinium Chelate: The Liver-Specific Magnetic Resonance Imaging Contrast Agent Gd-EOB-DTPA

H. Schmitt-Willich,* M. Brehm, Ch. L. J. Ewers, G. Michl, A. Müller-Fahrnow, O. Petrov, J. Platzek, B. Radüchel, and D. Sülzle

Research Laboratories of Schering AG, D-13342 Berlin, Germany

Received September 9, 1998

A convenient synthesis of disodium *S*-[4-(4-ethoxybenzyl)-3,6,9-tris[(carboxy- κ O)methyl]-3,6,9-triazaundecandioato)(5-)- κ^3 N³,N⁶,N⁹, κ^2 O¹,O¹¹]gadolate(2-) (Gd-EOB-DTPA), **1**, is reported. This water-soluble complex is presently undergoing phase III clinical trials as a liver-specific contrast agent for magnetic resonance imaging (MRI). The thermodynamic complex stability constant of **1** and the acid dissociation constants of the ligand have been determined as well as the stability constant of the calcium complex Ca-EOB-DTPA (**2**), which is used as an additive in the pharmaceutical formulation of the contrast agent. The solid-state structure of the ligand *S*-4-(4-ethoxybenzyl)-3,6,9-tris(carboxylatomethyl)-3,6,9-triazaundecanedioic acid (H₃EOB-DTPA), **3**, has been elucidated in a single crystal X-ray diffraction study. Additionally, HPLC evidence is given that the enantiomerically pure ligand forms two diastereomeric gadolinium complexes in a 65:35 ratio. The kinetics of isomerization of the isolated diastereomers—as dependent on pH and temperature—has been investigated, and thus, the activation energy for the interconversion of these isomers has been estimated to be 75.3 kJ mol⁻¹. Finally, the structures of the two components of **1** are discussed in terms of four possible diastereomers.

Introduction

Metal chelates containing highly paramagnetic gadolinium ions have been used effectively in clinical medicine to enhance contrast in magnetic resonance imaging (MRI) and thus to improve the efficacy of this diagnostic method.^{1–3} Up to the present day, gadolinium DTPA (Magnevist, Schering AG), which was approved in 1988 as the first MR contrast agent, has been used in more than 20 million patients. Aminopolycarboxylic acids such as diethylenetriamine pentaacetic acid (DTPA) and acetic acid derivatives of the macrocycle 1,4,7,10-tetraazacyclododecane form thermodynamically and/or kinetically very stable complexes with Gd(III)^{4–8} that can be used as contrast agents. However, the gadolinium chelates used so far in clinical practice are nonspecific contrast agents; i.e., after intravenous administration they are distributed in the extracellular water space of the body. Markedly different from Gd-DTPA is the pharmacodynamics of gadolinium ethoxybenzyl-DTPA, Gd-EOB-DTPA, **1** (international nonproprietary name: gadoxetic acid, disodium salt), which is presently undergoing clinical phase III studies.^{9–11} The specific uptake of **1** by the

hepatocytes but not by tumorous tissue allows the detection and differentiation of hepatic tumors.¹² In addition to its use in MRI, **1** has been tested successfully in patients as a potential contrast agent for computed tomography (CT).¹³

Several reports have appeared in the literature describing the synthesis and application of DTPA derivatives with lipophilic groups both in the acetic acid side chains¹⁴ and the diethylenetriamine backbone.^{15–18} Most of these papers deal with bifunctional ligands such as were first described in the pioneering work of Meares¹⁹ for EDTA derivatives. Interest in the attachment of radioactive metal ions to monoclonal antibodies for the diagnosis and treatment of cancer has, in particular, led to the development of such bifunctional agents. In addition, one gadolinium chelate²⁰ that was assumed—on the basis of animal data—to have the potential of a liver-specific MRI contrast agent

- (1) Brady, T. J.; Reimer, P. In *Encyclopedia of Nuclear Magnetic Resonance*; Grant, D. M., Harris, R. K., Eds.-in-Chief; John Wiley & Sons: New York, 1996; Vol. 3, pp 1432–38.
- (2) Brasch, R. C. *Radiology* **1992**, *183*, 1–11.
- (3) Lauffer, R. B. *Chem Rev.* **1987**, *87*, 901–927.
- (4) Aslanian, V.; Lemaigen, H.; Bunouf, P.; Svaland, M. G.; Borseth, A.; Lundby, B. *Neuroradiology* **1996**, *38*, 537–541.
- (5) Oudkerk, M.; Sijens, P. E.; Van Beek, E. J.; Kuijpers, T. J. *Invest Radiol.* **1995**, *30*, 75–78.
- (6) Kumar, K.; Chang, C. A.; Francesconi, L. C.; Dischino, D. D.; Malley, M. F.; Gougoutas, J. Z.; Tweedle, M. F. *Inorg. Chem.* **1994**, *33*, 3567–3575.
- (7) Platzek, J.; Blaszkiewicz, P.; Gries, H.; Luger, P.; Michl, G.; Müller-Fahrnow, A.; Radüchel, B.; Sülzle, D. *Inorg. Chem.* **1997**, *36*, 6086–6093.
- (8) Micskei, K.; Helm, L.; Brücher, E.; Merbach, A. E. *Inorg. Chem.* **1993**, *32*, 3844–3850.

- (9) Vogl, T. J.; Kümmel, S.; Hammerstingl, R.; Schellenbeck, M.; Schumacher, G.; Balzer, T.; Schwarz, W.; Müller, P. K.; Bechstein, W. O.; Mack, M. G.; Söllner, O.; Felix, R. *Radiology* **1996**, *200*, 59–67.
- (10) Schuhmann-Giampieri, G.; Schmitt-Willich, H.; Press, W.-R.; Negishi, C.; Weinmann, H.-J.; Speck, U. *Radiology* **1992**, *183*, 59–64.
- (11) Vander Elst, L.; Maton, F.; Laurent, S.; Seghi, F.; Chapelle, F.; Muller, R. N. *Magn. Reson. Med.* **1997**, *38*, 604–614.
- (12) Reimer, P.; Rummeny, E. J.; Shamsi, K.; Balzer, T.; Daldrup, H. E.; Tombach, B.; Hesse, T.; Berns, T.; Peters, P. E. *Radiology* **1996**, *199*, 177–183.
- (13) Schmitz, S. A.; Häberle, J. H.; Balzer, T.; Shamsi, K.; Boese-Landgraf, J.; Wolf, K.-J. *Radiology* **1997**, *202*, 399–405.
- (14) Williams, M. A.; Rapoport, H. *J. Org. Chem.* **1993**, *58*, 1151–1158.
- (15) Brechbiel, M. W.; Gansow, O. A. *Bioconjugate Chem.* **1991**, *2*, 187–194.
- (16) Westerberg, D. A.; Carney, P. L.; Rogers, P. E.; Kline, S. J.; Johnson, D. K. *J. Med. Chem.* **1989**, *32*, 236–243.
- (17) Brechbiel, M. W.; Gansow, O. A.; Atcher, R. W.; Schlom, J.; Esteban, J.; Simpson, D. E.; Colcher, D. *Inorg. Chem.* **1986**, *25*, 2772–2781.
- (18) Schmitt-Willich, H.; Platzek, J.; Gries, H.; Schuhmann-Giampieri, G.; Vogler, H.; Weinmann, H.-J. U.S. Patent No. 5,695,739, Dec 9, 1997 (Priority Jun 30, 1989); Eur. Pat. No. 0 405 704.
- (19) Meares, C. F.; Wensel, T. G. *Acc. Chem. Res.* **1984**, *17*, 202–209.

has been described. Surprisingly, the biliary elimination of this compound in humans was as low as 2–4%²¹ compared with approximately 50% of the injected dose that was found for **1**.¹²

Here we present for the first time (a) the detailed description of the synthesis of **1** including a convenient large-scale synthesis of the complex, (b) the protonation and stability constants, (c) evidence for the existence of at least two diastereomeric gadolinium complexes and their kinetics and thermodynamics of equilibration, and (d) the X-ray structure of the enantiomerically pure *S*-EOB ligand **3**.

Experimental Section

General Considerations. NMR spectra were obtained on a QE300 (300 MHz, General Electric), an AC400 (400 MHz, Bruker), or an AMX500 (500 MHz, Bruker). ¹H and ¹³C spectra were referenced to internal TMS (CDCl₃, DMSO) or TSP (D₂O). FT-IR spectra were recorded on a Nicolet 20SXB or on a Nicolet 710. Mass spectra were recorded on a VG ZAB-E or on a Fisons Autospec using FAB techniques with various matrices.

Synthesis. *O*-Ethyl-*N*_α-benzyloxycarbonyl-L-tyrosine methyl ester (5**) (Scheme 1).** To a solution of 658.7 g (2 mol) of *N*_α-benzyloxycarbonyl-L-tyrosine methyl ester (**4**)²² in 4.5 L of dimethylformamide was added 552.9 g (4 mol) of powdered potassium carbonate, followed by 177 mL (2.2 mol) of ethyl iodide. After being stirred overnight at room temperature, the reaction mixture was evaporated under reduced pressure. The residue was dissolved in 2.5 L of ethyl acetate and 1.5 L of water, the organic layer was washed with water, dried with sodium sulfate, and filtrated, and the filtrate was evaporated to yield 700 g (98%) of **5**. Mass spectrum (FAB): *m/e* 358 [(M + H)⁺]. [α]_D²⁰ = -17.2° (*c* = 1, methanol). Mp: 52–54 °C. ¹H NMR (300 MHz) (CDCl₃) δ: 1.40 (t (7 Hz), 3H), 2.96–3.13 (m, 2H), 3.70 (s, 3H), 4.00 (q (7 Hz), 2H), 4.57–4.67 (m, 1H), 4.03–5.15 (m, 2H), 5.22 (d (7 Hz), 1H), 6.77–6.84 (m, 2H), 6.95–7.02 (m, 2H), 7.27–7.51 (m, 5H). Infrared spectrum (KBr, cm⁻¹): 3340; 3020; 2980; 2960; 2950; 2930; 2900; 1745; 1695; 1630; 1580; 1530; 1520; 1480; 1470; 1455; 1440; 1390; 1340; 1330; 1320; 1290; 1255; 1245; 1215; 1180; 1170; 1150; 1120; 1070; 1050; 1020; 920; 845; 840; 810; 760; 730; 700. Anal. Calcd (found) for C₂₀H₂₃NO₅: C, 67.21 (67.17); H, 6.49 (6.26); N, 3.92 (3.82).

***N*-(2-Aminoethyl)-*N*_α-benzyloxycarbonyl-*O*-ethyl-L-tyrosinamide Hydrochloride (**6**) (Scheme 1).** A solution of 679 g (1.9 mol) of **5** in 1.2 L of methanol was added dropwise to 2.6 L of ethylenediamine over a period of 5 h. The solution was stirred at room temperature for 20 h and concentrated in vacuo. Immediately after evaporation, the oily residue was dissolved in 4.5 L of methyl *tert*-butyl ether (MTBE) and stirred overnight. The amorphous colorless precipitate was collected by filtration, washed with approximately 0.5 L of MTBE, and dried in vacuo at 40 °C. The residue was then suspended in 5 L of water and stirred overnight at room temperature. The solid was collected by filtration and washed well with approximately 2 L of water to remove traces of ethylenediamine. The residue was dried in vacuo at 40 °C and then dissolved in 1.1 L of methanol at 50 °C. After the solution was cooled to room temperature, 159 mL (1.9 mol) of concentrated HCl was added. The precipitate was filtered off, washed with cold ethanol, and dried in vacuo at 50 °C. Yield: 555.3 g (69.3%). Mass spectrum (FAB): *m/e* 386 [(M + H)⁺]. [α]_D²⁰ = -7.3° (*c* = 1, glacial acetic acid). Mp: 210–212 °C. ¹H NMR (300 MHz) (DMSO-*d*₆) δ: 1.30 (t (7 Hz), 3H), 2.50–3.20 (m, 8H), 3.96 (q (7 Hz), 2H), 4.08–4.12 (m, 1H), 4.88–5.02 (m, 2H), 6.78 (d (8 Hz), 2H), 7.15 (d (8 Hz), 2H), 7.20–7.50 (m, 5H) 7.42 (d (8 Hz), 1H), 7.94 (t (5 Hz), 1H). Infrared spectrum (KBr, cm⁻¹): 3300; 3090; 3060; 3040; 2980; 2940; 2880; 1720; 1650; 1600; 1570; 1550; 1540;

1480; 1450; 1430; 1380; 1280; 1260; 1250; 1150; 1140; 1050; 1040; 940. Anal. Calcd (found) for C₂₁H₂₇N₃O₄·HCl: C, 59.78 (59.79); H, 6.45 (6.48); Cl, 8.40 (8.53); N, 9.96 (10.07).

***N*-(2-Aminoethyl)-*O*-ethyl-L-tyrosinamide (**7**) (Scheme 1).** **6** (278.5 g, 660 mmol) was suspended in 2.4 L of methanol. Approximately 40 g of Pd (10%) on charcoal was added under nitrogen, and the mixture was hydrogenated in a 5 L autoclave at 15 atm hydrogen pressure at room temperature for 6 h. After addition of 55 mL of concentrated HCl to the suspension, the catalyst was filtered off and the filtrate was evaporated to dryness. Toluene (1.5 L) and 300 mL of 50% aqueous KOH were added to the oily residue, and the mixture was warmed to 70 °C until the oil was being dissolved. The organic phase was separated, and the aqueous phase was extracted three times with 1 L of toluene each. The combined toluene layers were dried with KOH and filtered, and the filtrate was evaporated under reduced pressure to yield 143 g (86%) of **7** as a light yellow oil. It was used in the next step without further purification. An analytical sample was characterized as dihydrochloride. Mass spectrum (FAB): *m/e* 252 [(M + H)⁺]. [α]_D²⁰ = +84.9° (*c* = 1, methanol). Mp: 87–89 °C. ¹H NMR (400 MHz) (MeOD) δ: 1.37 (t (7 Hz), 3H), 2.95–3.22 (m, 4H), 3.36 (t (6 Hz), 1H), 3.57–3.65 (m, 1H), 4.02 (q (7 Hz), 2H), 4.10 (t (6 Hz), 1H), 4.60–5.10 (broad, 7H), 6.85–6.93 (m, 2H), 7.17–7.26 (m, 2H). Infrared spectrum (KBr, cm⁻¹): 3480; 3200; 3049; 2980; 1680; 1675; 1615; 1520; 1515; 1400; 1370; 1310; 1300; 1250; 1190; 1180; 1120; 1050. Anal. Calcd (found) for C₁₃H₂₁N₃O₂·2 HCl: C, 48.16 (48.34); H, 7.15 (6.96); N, 12.96 (12.63); Cl, 21.87 (21.66).

***S*-1-(4-Ethoxybenzyl)-3-azapentane-1,5-diamine Trihydrochloride (**8a**) (Scheme 1).** *N*-(2-Aminoethyl)-*O*-ethyl-L-tyrosinamide (**7**) (143 g, 569 mmol) was dissolved in 4.8 L (4.8 mol) of borane–tetrahydrofuran complex (1.0 M in tetrahydrofuran). The solution was concentrated in vacuo to a volume of approximately 2 L and refluxed for 32 h at a bath temperature of 80 °C. The solution was then cooled to 0 °C, and 250 mL of methanol was added slowly within 30 min. After 2 h at 0 °C, gaseous HCl was bubbled through the solution until the pH was distinctly acidic. The resulting suspension was stirred for 2 h, and the precipitate was collected by filtration, washed with a total of 2.5 L of tetrahydrofuran, and dried in vacuo at room temperature over P₂O₅. Yield: 185 g (94%). Mass spectrum (FAB): *m/e* 238 [(M + H)⁺]. [α]_D²⁰ = -10.7° (*c* = 1, methanol). Mp: 170 °C dec. ¹H NMR (300 MHz) (MeOD) δ: 1.38 (t (7 Hz), 3H), 3.03 (dd (14, 7 Hz), 1H), 3.15 (dd (14, 6 Hz), 1H), 3.35–3.62 (m, 6H), 3.95–4.10 (m, 3H), 6.88–6.98 (m, 2H), 7.23–7.36 (m, 2H), 8–9 (br, >6H). ¹³C NMR (DMSO-*d*₆) δ: 14.59 (q); 34.93 (t); 35.14 (t); 44.26 (t); 47.83 (t); 49.41 (d); 62.84 (t); 114.50 (d); 126.79 (s); 130.44 (d); 157.57 (s). Infrared spectrum (KBr, cm⁻¹): 3430; 2200–3300 (broad); 1630; 1580; 1530; 1480; 1460; 1440; 1395; 1305; 1250; 1180; 1130; 1050; 980; 920; 810. Anal. Calcd (found) for C₁₃H₂₃N₃O·3 HCl: C, 45.03 (45.32); H, 7.56 (6.67); Cl, 30.67 (29.31); N, 12.12 (12.08).

Benzyl *N*-[*S*-1-(4-Ethoxybenzyl)-2-hydroxyethyl]carbamate (9**) (Scheme 2).** Sodium borohydride (14.8 g, 391.7 mmol) was added to a solution of 100.0 g (279.8 mmol) of *O*-ethyl-*N*_α-benzyloxycarbonyl-L-tyrosine methyl ester (**5**) in 700 mL of tetrahydrofuran. Then 125 mL of methanol was slowly added to the resulting suspension and the temperature kept below 30 °C. After the mixture was stirred for 1 h at room temperature, the excess reagent was destroyed by addition of 21.6 mL of acetic acid. The solvent was evaporated, and the oily residue was diluted with 1 L of water and extracted three times with 0.5 L of ethyl acetate each. The combined organic extracts were washed with brine, dried with sodium sulfate, and concentrated in vacuo. Crystallization from hexane/ethyl acetate (2:1) yielded 85.2 g (92.5%) of **9** as white crystals. Mass spectrum (FAB): *m/e* 330 [(M + H)⁺]. [α]_D²⁰ = -171.5° (*c* = 1, methanol). Mp: 101–104 °C.

¹H NMR (400 MHz) (MeOD) δ: 1.35 (t (7 Hz), 3H), 2.62 (dd (14, 8 Hz), 1H), 2.82 (dd (14, 5 Hz), 1H), 3.46–3.57 (m, 2H), 3.75–3.85 (m, 1H), 3.95 (q (7 Hz), 2H), 4.96 (d (12 Hz), 1H), 5.03 (d (12 Hz), 1H), 6.74–6.82 (m, 2H), 7.05–7.13 (m, 2H), 7.21–7.33 (m, 5H). ¹³C NMR (MeOD): 15.29 (q); 37.52 (t); 56.14 (d); 64.45 (t); 64.55 (t); 67.23 (t); 115.44 (d); 128.64 (d); 128.86 (d); 129.43 (d); 131.31 (d); 131.78 (s); 138.45 (s); 158.52 (s); 158.93 (s). Infrared spectrum (KBr, cm⁻¹): 3460; 3430; 3360; 3310; 3080; 3040; 2980; 2960; 2930; 2840; 1700; 1690; 1670; 1665; 1610; 1570; 1595; 1590; 1510; 1480; 1455;

(20) Uggeri, F.; Aime, S.; Anelli, P. L.; Botta, M.; Brocchetta, M.; de Haen, C.; Ermondi, G.; Grandi, M.; Paoli, P. *Inorg. Chem.* **1995**, *34*, 633–642.

(21) Vogl, T. J.; Stupavsky, A.; Pegios, W.; Hammerstingl, R.; Mack, M.; Diebold, T.; Lodemann, K.-P.; Neuhaus, P.; Felix, R. *Radiology* **1997**, *205*, 721–728.

(22) Kinoshita, M.; Klostermeyer, H. *Liebigs Ann. Chem.* **1966**, *696*, 226.

1395; 1350; 1330; 1300; 1265; 1250; 1180; 1140; 1115; 1080; 1075; 1050; 1040; 1030; 960; 925; 740. Anal. Calcd (found) for $C_{19}H_{23}NO_4$: C, 69.28 (68.93); H, 7.04 (7.27); N, 4.25 (3.96).

Benzyl N-[S-1-(4-Ethoxybenzyl)-2-mesyloxyethyl]carbamate (10) (Scheme 2). Methanesulfonyl chloride (20.86 mL, 267.8 mmol) was added at 0 °C to a solution of 84.0 g (255.0 mmol) of **9** and 37.82 mL (272.9 mmol) of triethylamine in 330 mL of tetrahydrofuran. The reaction mixture was stirred for 30 min at room temperature, and the triethylamine hydrochloride was removed by filtration. The solid was carefully washed four times with 15 mL of tetrahydrofuran. The combined filtrates that contained the crude mesylate were used directly in the next step without further purification. An analytical sample of **10** was obtained by crystallization from water/tetrahydrofuran. Mass spectrum (FAB): m/e 408 [(M + H)⁺]. $[\alpha]_D^{20} = -48.5^\circ$ ($c = 1$, methanol). Mp: 104–106 °C.

¹H NMR (300 MHz) (CDCl₃) δ : 1.40 (t (7 Hz), 3H), 2.70–2.90 (m, 2H), 2.98 (s, 3H), 4.01 (q (7 Hz), 2H), 4.05–4.20 (m, 2H), 4.20–4.30 (m, 1H), 4.94 (d (6 Hz), 1H), 5.10 (s, 2H), 6.80–6.87 (m, 2H), 7.05–7.15 (m, 2H), 7.30–7.42 (m, 5H). Infrared spectrum (KBr, cm⁻¹): 3340; 3080; 3040; 2980; 2940; 1695; 1610; 1580; 1745; 1510; 1450; 1445; 1400; 1350; 1335; 1270; 1245; 1180; 1020; 1170; 1050; 980; 855; 840. Anal. Calcd (found) for $C_{20}H_{25}NO_6S$: C, 58.95 (58.96); H, 6.18 (6.55); N, 3.44 (3.44); S, 7.87 (7.34).

Benzyl N-[S-2-(2-Aminoethylamino)-1-(4-ethoxybenzyl)ethyl]carbamate, Dihydrochloride (11) (Scheme 2). Ethylenediamine (420 mL, 6375 mmol, 25 equiv) was added to the above mesylate solution. The reaction mixture was stirred at 50 °C for 4 h. After evaporation of the tetrahydrofuran and most of the excess ethylenediamine under reduced pressure, the mixture was diluted with 200 mL of water and extracted three times with 300 mL of ethyl acetate each. The combined organic extracts were washed with water, dried with sodium sulfate, and concentrated in vacuo. The residue was dissolved in a mixture of methanol/MTBE (1:1) and acidified with concentrated HCl. The precipitate was collected by filtration, washed with MTBE, and dried at 50 °C to yield 91.86 g (81%) of **11** as a white solid. Mass spectrum (FAB): m/e 372 [(M + H)⁺]. $[\alpha]_D^{20} = -42^\circ$ ($c = 1$, methanol). Mp: 208–212 °C dec. ¹H NMR (500 MHz) (MeOD) δ : 1.37 (t (7 Hz), 3H), 2.77 (dd (14, 9 Hz), 1H), 2.84 (dd (14, 5 Hz), 1H), 3.21 (t (12 Hz), 1H), 3.25 (dd (12, 3 Hz), 1H), 3.30–3.48 (m, 4H), 3.99 (q (7 Hz), 2H), 4.08–4.18 (m, 1H), 4.98 (d (12 Hz), 1H), 5.10 (d (12 Hz), 1H), 6.79–6.84 (m, 2H), 7.10–7.17 (m, 2H), 7.22–7.37 (m, 5H). Infrared spectrum (KBr, cm⁻¹): 3310; 3200; 2400–3100; 1710; 1610; 1580; 1535; 1510; 1480; 1450; 1460; 1310; 1275; 1265; 1245; 1170; 1140; 1120; 1065; 990; 980; 685. Anal. Calcd (found) for $C_{21}H_{29}N_3O_3 \cdot 2HCl$: C, 56.76 (57.06); H, 7.03 (7.18); Cl, 15.96 (15.83); N, 9.46 (9.01).

S-1-(4-Ethoxybenzyl)-3-azapentane-1,5-diamine Dihydrochloride (8b) (Scheme 2). A solution of 90.0 g (202.53 mmol) of **11** in 2.7 L of methanol was hydrogenated over 10% Pd on charcoal at 15 bar for 1 h at room temperature. The catalyst was filtered off, and the solvent was evaporated under reduced pressure. Crystallization from methanol/MTBE (1:4) yielded 56.86 g (92.5%) of **8b** as a white solid. Mass spectrum (FAB): m/e 238 [(M + H)⁺]. $[\alpha]_D^{20} = +15.8^\circ$ ($c = 1$, methanol). Mp: 220–225 °C dec. ¹H NMR (300 MHz) (MeOD) δ : 1.36 (t (7 Hz), 3H), 2.68 (dd (12, 9 Hz), 1H), 2.75–3.15 (m, 7H), 3.42–3.56 (m, 1H), 4.02 (q (7 Hz), 2H), 6.85–6.93 (m, 2H), 7.17–7.25 (m, 2H). Infrared spectrum (KBr, cm⁻¹): 3440; 3280; 3100; 3040; 2980; 2940; 2880; 2580; 1610; 1580; 1510; 1480; 1390; 1300; 1250; 1230; 1180; 1140; 1110; 1050; 920; 850; 800. Anal. Calcd (found) for $C_{13}H_{23}N_3O \cdot 2HCl$: C, 50.33 (50.60); H, 8.12 (8.30); N, 13.54 (13.30); Cl 22.85 (23.00).

Di-tert-butyl S-4-(4-Ethoxybenzyl)-3,6,9-tris(tert-butoxycarbonylmethyl)-3,6,9-triazaundecandioate (12) (Scheme 3). Triamine dihydrochloride **8b** (108.58 g, 350 mmol) was suspended in 3.5 L of tetrahydrofuran. After addition of 241.9 g (1.75 mol) of potassium carbonate and 175 mL of water, 512 g (2.625 mol) of *tert*-butyl bromoacetate was dropped into the reaction mixture and then refluxed for 20 h. The resulting triphasic system was cooled to room temperature, the solid was filtered off, the aqueous phase (small volume) was removed by a separatory funnel, and the organic phase was concentrated in vacuo. The residue was chromatographed on Kromasil RP 8, 10 μ m

(methanol/water/ammonia 9/1/0.1), and **12** was isolated from the collected fractions by extraction with methyl *tert*-butyl ether to yield 206.4 g (73%) of **12** as a light yellow oil. (Starting with trihydrochloride **8a** instead of **8b**, the same procedure was applied but 266.1 g (1.925 mol) of potassium carbonate was used for the alkylation of 350 mmol of **8a**). Mass spectrum (FAB): m/e 809 [(M + H)⁺]. $[\alpha]_D^{20} = -5.3^\circ$ ($c = 1$, methanol). ¹H NMR (500 MHz) (pyridine-*d*₅) δ : 1.28 (t (7 Hz), 3H), 1.44–1.52 (s, 45H), 2.84 (dd (14, 6 Hz), 1H), 2.90 (dd (14, 6 Hz), 1H), 3.03–3.17 (m, 5H), 3.21 (dd (14, 6 Hz), 1H), 3.43–3.50 (m, 1H), 3.70–3.84 (m, 10H), 3.92 (q (7 Hz), 2H), 6.97–7.01 (m, 2H), 7.40–7.43 (m, 2H); Infrared spectrum (KBr, cm⁻¹) 2980; 2930; 1740; 1610; 1510; 1480; 1460; 1430; 1390; 1375; 1290; 1245; 1220; 1150. Anal. Calcd (found) for $C_{43}H_{73}N_3O_{11}$: C, 63.91 (64.14); H, 9.11 (9.35); N, 5.20 (5.10).

S-4-(4-Ethoxybenzyl)-3,6,9-tris(carboxylatomethyl)-3,6,9-triazaundecandioic Acid, Nonstoichiometric Sodium Salt (EOB-DTPA Sodium Salt) (13) (Scheme 3). NaOH (45 g, 1.125 mol) in 62.5 mL of water was added to a solution of 101.0 g (125 mmol) of **12** in 750 mL of methanol. The solution was refluxed for 5 h and stirred at room temperature overnight. Methanol was evaporated, the residue diluted with water, and the solution adjusted to pH 3.0 using the cation-exchange resin Amberlite IR 120 (H⁺ form). According to the protonation constants of **3** (see Results and Discussion) the solution contains at pH 3.0 approximately 3% (H₂EOB-DTPA)³⁻, 64% (H₃-EOB-DTPA)²⁻, 30% (H₄EOB-DTPA)⁻, and 3% H₅EOB-DTPA. The resin was removed by filtration, and the filtrate containing 66.3 g (94.0%) of **13** was used in the following complexation step without isolation. An analytical sample was lyophilized to give EOB-DTPA sodium salt **13** as a white amorphous powder. Mass spectrum (FAB): m/e 528 [(H₅EOB-DTPA + H)⁺], 550 [(NaH₄EOB-DTPA + H)⁺], 572 [(Na₂H₃EOB-DTPA + H)⁺], 594 [(Na₃H₂EOB-DTPA + H)⁺], 616 [(Na₄H₁EOB-DTPA + H)⁺], 638 [(Na₅EOB-DTPA + H)⁺], 660 [(Na₅-EOB-DTPA + Na)⁺]. $[\alpha]_D^{20} = +10.6^\circ$ ($c = 1$, water). Mp: 220–230 °C dec. ¹H NMR (400 MHz) (D₂O) δ : 1.38 (t (7 Hz), 3H), 2.80 (dd (14, 8 Hz), 1H), 2.98–3.18 (m, 5H), 3.32–3.52 (m, 5H), 3.65–3.88 (m, 9H), 4.12 (q (7 Hz), 2H), 6.96–7.03 (m, 2H), 7.21–7.28 (m, 2H). Infrared spectrum (KBr, cm⁻¹): 3440; 3030; 3010; 2980; 2930; 2880; 2440br; 1900br; 1715br; 1630br; 1520; 1470; 1400; 1310; 1245; 1180; 1115; 1090; 1050; 980; 920; 910; 840; 810; 700. Anal. Calcd (found) for $C_{23}H_{31.33}N_3Na_{1.67}O_{11}$: C, 48.96 (48.71); H, 5.60 (5.51); N, 7.45 (7.16); Na, 6.80 (6.67).

Disodium S-[4-(4-Ethoxybenzyl)-3,6,9-tris(carboxy-*k*O)methyl]-3,6,9-triazaundecandioate(5-)- $\kappa^3N^3, N^6, N^9, \kappa^2O^1, O^{11}$] gadolinate(2-) (Gadolinium-EOB-DTPA) (Gadoxetic Acid, Disodium Salt) (**1**) (Scheme 3). To a solution of 152.3 g (270 mmol) of **13** in 1.5 L of water was added 48.94 g (135 mmol) of Gd₂O₃. The mixture was stirred at 80 °C for 1 h. The solution was filtered at room temperature through a 0.2 μ m filter, and the pH was adjusted to 7.0 using approximately 90 mL (90 mmol) of 1 N NaOH. The solution was concentrated in vacuo to a volume of approximately 150 mL and diluted with the 3-fold amount of ethanol. This mixture was added slowly at 50 °C to 2.4 L of ethanol. After the mixture was heated under reflux for 2 h, the precipitate was collected by filtration, washed with 1.5 L of ethanol/water (95:5), and dried in vacuo at 50 °C to yield 167 g (85.2%) of **1** as a white powder. HPLC: Hypersil ODS 3 μ m, column length 12.5 cm, diameter 4.6 mm; mobile phase, 250 mL of acetonitrile/100 mL of 0.1 M aqueous tetrabutylammonium hydroxide/650 mL of water (pH 8.4), flow rate 1 mL/min, UV detection at 196 nm. Mass spectrum (FAB): m/e 727 [(M + H)⁺]. $[\alpha]_D^{20} = +27.0^\circ$ ($c = 1$, methanol). Mp: >300 °C. Infrared spectrum (KBr, cm⁻¹): 2980; 3440; 2990; 2920; 1605; 1510; 1475; 1400; 1325; 1275; 1240; 1180; 1115; 1090; 990; 975; 925. Anal. Calcd (found) for $C_{23}H_{28.25}GdN_3Na_{1.75}O_{11}$: C, 38.36 (38.27); H, 3.95 (3.70); Gd, 21.83 (21.08); N, 5.83 (5.78); Na, 5.59 (5.50).

Disodium S-[4-(4-Ethoxybenzyl)-3,6,9-tris(carboxy-*k*O)methyl]-3,6,9-triazaundecandioate(5-)- $\kappa^3N^3, N^6, N^9, \kappa^2O^1, O^{11}$] lanthanoate(2-) (La-EOB-DTPA). To a solution of 1.52 g (2.7 mmol) of **13** in 15 mL of water was added 440 mg (1.35 mmol) of La₂O₃. The mixture was stirred at 90 °C for 24 h. After the mixture was cooled to room temperature, the pH was adjusted to 7.0 with diluted NaOH, and then the solution was filtered through a 0.2 μ m filter and lyophilized to

Table 1. Crystal Data and Structure Refinement for H₅EOB-DTPA **3**

empirical formula	C ₂₃ H ₃₃ N ₃ O ₁₁ ·4H ₂ O
crystal size (mm ³)	0.6 × 0.15 × 0.1
crystal system, space group	monoclinic, P2 ₁
unit cell dimensions	<i>a</i> = 10.328(4) Å <i>b</i> = 8.053(3) Å <i>c</i> = 17.490(8) Å <i>β</i> = 95.54(4)°
<i>Z</i>	2
formula weight	527.5 g/mol
density (calcd)	1.375 Mg/m ³
absorption coefficient <i>F</i> (000)	0.116 mm ⁻¹ 640
diffractometer used	Siemens P4
radiation	Mo Kα (<i>λ</i> = 0.71073 Å)
<i>T</i> (K)	294
monochromator	highly oriented graphite crystal
2θ range	3.0–47.5°
scan type and range	<i>ω</i> , 1.20° plus Kα separation
scan speed	variable (1.9 to 59°/min in <i>ω</i>)
index ranges	−11 < <i>h</i> < 11, −9 < <i>k</i> < 9, −19 < <i>l</i> < 19
reflections collected	8593
independent reflections	4414 (<i>R</i> _{int} = 5.4%)
observed reflections	3132 (<i>F</i> > 4.0σ(<i>F</i>))
absolute structure	<i>η</i> = 0.84(16)
quantity minimized	Σ <i>ω</i> (<i>F</i> _o − <i>F</i> _c) ²
hydrogen atoms	riding model, two common <i>U</i> 's for hydrogen atoms
final <i>R</i> Indices (obsd data)	<i>R</i> = 5.7%, <i>R</i> _w = 4.5%
<i>R</i> indices (all data)	<i>R</i> = 8.0%, <i>R</i> _w = 4.8%
goodness-of-fit	1.73
data-to-parameter ratio	8.4:1
largest difference peak and hole	0.60 e Å ⁻³ , −0.39 e Å ⁻³

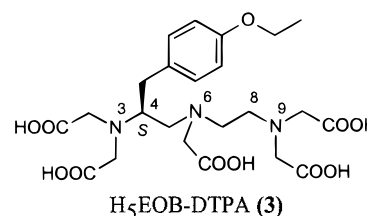
yield 1.85 g (97%) of La-EOB-DTPA as a white powder. Mass spectrum (FAB): *m/e* 708 [(M + H)⁺]. [α]_D²⁰ = +27.7° (*c* = 1, methanol). Mp: > 300 °C. ¹H NMR (500 MHz) (D₂O) δ: δ 1.38–1.43 (m), 2.02 (d (14 Hz)), 2.24 (d (14 Hz)), 2.48–2.81 (m), 2.86–3.38 (m), 3.40–3.62 (m), 3.73–3.89 (m), 4.10–4.20 (m), 7.00–7.06 (m), 7.23–7.30 (m). Two overlapping data sets can be identified with a molar ratio of 60:40. ¹³C NMR (D₂O) δ: 16.8 (q); 32.6 (t); 34.1 (t); 57.6 (t); 58.2 (t); 59.7 (t); 59.9 (t); 61.1 (t); 62.5 (t); 64.0 (t); 65.1 (t); 65.3 (t); 66.3 (t); 66.5 (d); 67.0 (t); 67.2 (t); 68.2 (t); 117.8 (d); 117.9 (d); 133.1 (d); 133.2 (d); 134.1 (s); 159.4 (s); 159.5 (s); 182.6 (s); 182.9 (s); 183.6 (s); 183.6 (s); 183.8 (s); 183.9 (s); 184.0 (s). Infrared spectrum (KBr, cm⁻¹): 3440br; 2930; 2980; 1610; 1510; 1400; 1330; 1245; 1170; 1130; 1090; 920. Anal. Calcd (found) for C₂₃H_{28.25}LaN₃Na_{1.75}O₁₁: C, 39.36 (39.47); H, 4.06 (4.16); La, 19.79 (19.87); N, 5.99 (5.72); Na, 5.73 (5.55).

S-4-(4-Ethoxybenzyl)-3,6,9-tris(carboxylatomethyl)-3,6,9-triazaundecandioic Acid, Calcium Complex, Trisodium Salt (Calcium-EOB-DTPA) (2) (Scheme 3). To a solution of 4.51 g (8 mmol) of **13** in 100 mL of water was added 0.59 g (8 mmol) of Ca(OH)₂, and the mixture was stirred at room temperature for 20 min. With diluted NaOH the pH was adjusted to 7.0, and the solution was filtered through a 0.2 μm filter and lyophilized to yield 4.9 g (97.8%) of **2** as a white powder. Mass spectrum (FAB): *m/e* 632 [(M + H)⁺]. [α]_D²⁰ = +10.7° (*c* = 3, water). Mp: 275 °C dec. ¹H NMR (500 MHz) (D₂O) δ: 1.38–1.46 (m, 3H), 1.7–3.8 (m, 19H), 4.08–4.15 (m, 2H), 6.90–6.98 (m, 2H), 7.18–7.25 (m, 2H). ¹³C NMR (D₂O) δ: 14.76 (q); 31.36 (t); 32.35 (t); 54.71 (t); 55.16 (t); 55.99 (t); 57.34 (t); 57.56 (t); 57.63 (t); 58.21 (t); 60.29; 61.70 (t); 62.20 (t); 62.34 (t); 64.38 (d); 46.87 (d); 65.13 (t); 65.18 (t); 115.64 (d); 115.69 (d); 131.08 (d); 131.11 (d); 132.70 (s); 132.75 (s); 157.15 (s); 157.23 (s); 180.58 (s); 180.65 (s); 180.78 (s); 181.21 (s); 181.36 (s). Infrared spectrum (KBr, cm⁻¹): 3420; 2980; 2940; 2860; 2840; 1600; 1520; 1420; 1380; 1250; 1180; 1120; 975; 925. Anal. Calcd (found) for C₂₃H₂₈CaN₃Na₃O₁₁: C, 43.74 (43.36); H, 4.47 (4.24); Ca, 6.35 (6.68); N, 6.65 (6.33); Na, 10.92 (10.12).

S-4-(4-Ethoxybenzyl)-3,6,9-tris(carboxylatomethyl)-3,6,9-triazaundecandioic Acid (H₅EOB-DTPA) (3) (Scheme 3). **13** (14.1 g, 25 mmol) in 50 mL of water was passed down a column of Amberlite IR

120 (35 mL, H⁺ form). The acidic eluate containing the product was filtered through a 0.2 μm filter and lyophilized to yield 12.1 g (91.8%) of **3**. To obtain crystals suitable for X-ray diffraction, aqueous solutions of **3** were prepared in different concentrations. In most of the setups, small crystals grew upon evaporation of the water. This solid material was used for new crystallization setups under similar conditions. Although the crystal size could thus be improved, growth of specimen suitable for diffraction data collection could only be achieved by seeding. One of the biggest crystals (0.6 × 0.15 × 0.1 mm³) was mounted on a glass rod and used for the X-ray single-crystal structure determination described below. Mass spectrum (FAB): *m/e* 528 [(M + H)⁺]. [α]_D²⁰ = +11.0° (*c* = 1, methanol). Mp: 200–210 °C dec. ¹H NMR (400 MHz) (DMSO-*d*₆) δ: 1.31 (t (7 Hz), 7 Hz), 2.47 (dd (14, 7 Hz), 1H), 2.78–2.90 (m, 4H), 2.90–3.10 (m, 3H), 3.2–3.50 (m, 9H), 3.60–3.75 (m, 2H), 3.99 (q (7 Hz), 2H), 6.80–6.85 (m, 2H), 7.10–7.15 (m, 2H), 8–12 (m, 5H). ¹³C NMR (DMSO-*d*₆) δ: 14.87 (q); 33.66 (t); 50.23 (t); 53.30 (t); 54.36 (t); 54.70 (t); 55.10 (t); 61.03 (d); 63.00 (t); 114.47 (d); 130.16 (d); 130.47 (s); 157.13 (s); 169.66 (s); 172.57 (s); 173.56 (s). Infrared spectrum (KBr, cm⁻¹): 3580; 3430; 3020; 3000; 2990; 2980; 2960; 2910; 2580br; 1900br; 1730; 1710; 1640; 1610; 1510; 1430; 1380; 1360; 1260; 1240; 1170; 1150; 1120; 1030; 1010; 980; 960; 920; 900. Anal. Calcd (found) for C₂₃H₃₃N₃O₁₁: C, 52.36 (52.13); H, 6.31 (6.16); N, 7.97 (7.93).

Collection and Reduction of X-ray Diffraction Intensity Data of 3. Details concerning the measurement of the intensity data and the structure determination are given in Table 1. The unit cell dimensions



(*a* = 10.328(4) Å, *b* = 8.053(3) Å, *c* = 17.490(8) Å, *β* = 95.54(4)°, monoclinic, space group P2₁, one molecule of **3** and four water molecules per asymmetric unit) were derived from the positions of 24 centered reflections with 6.98 < 2θ < 24.06°. The standard deviations of the unit cell axes and angles are within the usual range. To improve the quality of the intensity data, 4179 symmetry-equivalent reflections have been measured and merged (*R*_{int} = 5.4%). The mean ratio *I*/σ(*I*) of the data set with a maximum resolution of 0.88 Å is 8.31. Overall, 71% of the intensity data were considered as observed (*F* > 4.0σ(*F*)). The data were corrected for Lorentz and polarization effects, but no absorption correction has been applied. The quality of the intensity data is sufficient to determine and refine the crystal structure of **3** unambiguously.

Crystal Structure Solution and Refinement for 3. All calculations were performed using the Siemens SHELXTL+ (VMS)²³ program package. The structure was solved by direct methods and subsequent Fourier syntheses. The crystals belong to the monoclinic space-group P2₁. Four additional maxima in the electron density map were interpreted as water positions. After convergence was achieved for the anisotropic refinement, the hydrogen atoms bound to carbon atoms were included in calculated positions. One overall temperature factor was refined for these hydrogen atoms. The remaining hydrogen atoms belonging to the hydroxyl groups were located from a series of subsequently calculated difference Fourier maps. A second overall temperature factor was refined for this group of hydrogen atoms. The refinement converged at *R* = 5.73% (data to parameter ratio 8.4:1).

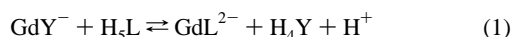
Potentiometric Equipment and Measurements. All reagents used for the pH-potentiometric studies were of highest analytical grade quality unless otherwise stated. Standard acid or base solutions were prepared by Titrisol ampules (Merck) or ready-for-use solutions were used. The CO₂ content of the standard base (0.1 M KOH) was monitored by titration of H₃PO₄ to be < 1%. The 0.1 M KCl solutions used as supporting electrolyte were prepared with KCl of Suprapur quality

(23) SHELXTL PLUS, Siemens Analytical X-ray Instruments, Inc.

(Merck). Stock solutions of GdCl_3 and CaCl_2 were prepared from $\text{GdCl}_3 \cdot 6\text{H}_2\text{O}$ (Ventron, 99.9% related to total rare earth content) and $\text{CaCl}_2 \cdot 4\text{H}_2\text{O}$ (Merck, Suprapur) and standardized by complexometric titrations. Solutions of **3** as well as solutions of EDTA or DTPA used in competition experiments or for comparison purposes were standardized by pH-potentiometric titrations of the ligands alone or in the presence of an excess of Ca(II) or Gd(III) ions. The pH-potentiometric measurements were made with a PC controlled titration system (Schott TPC 2000) in combination with an Ingold pH-electrode LoT 401-60-S7. The sealed titration cells (10 or 50 mL) were thermostated at 25 ± 0.1 °C by circulating water through the water jacket. The headspace of the vessels was purged with N_2 (after passing traps with 0.1 M KOH and 0.1 M KCl) during the measurements. All test solutions were prepared to be 0.1 M with KCl. The titrations were made under the most sensitive drift control with a minimum delay time between addition of base and measurement of 120 s.

The pH-electrode was calibrated in $-\log[\text{H}^+]$ units by titrations of 50 mL aliquots of 0.002 M HCl in 0.1 M KCl with standard base. Slope and standard potential E_0 of the glass electrode were obtained by linear regression calculations of the measured electrode potentials in mV versus the corresponding $-\log[\text{H}^+]$ (from the calculated titration curve) using six data points, each in the acidic and basic buffer regions of the titration curves (correlation factors were $r^2 = 1.000$). These calibration data were checked during the course of the study and slightly adjusted as necessary. Thus, in this study pH means $\text{p[H]} = -\log[\text{H}^+]$ and all equilibrium constants are concentration constants. The value used for the ion product of water is $\log K_w = 13.78$.²⁴

The protonation constants of **3** were determined in six pH-potentiometric titrations of 55 mL aliquots of approximately 1 mM solutions of **3** with 0.1 M KOH in 20 μL steps. The stability constants and protonation constants of the Ca complexes of EOB-DTPA were derived from analogous titration in the presence of Ca(II) at molar ratios Ca(II):EOB-DTPA of 1:1, 2:1, 3:1, and 6:1. The stability constant of **1** could not be determined in direct titrations of the ligand in the presence of Gd(III) because the degree of complexation was too high, even at low pH. Therefore, a competition method according to the following overall equilibrium with $\text{Y} = \text{EDTA}$ and $\text{H}_5\text{L} = \text{EOB-DTPA}$ was used:



Millimolar solutions of **3** were titrated in the presence of Gd(III) and EDTA at molar ratios Gd(III):3:EDTA of 1:1:2 and 1:1:4 (two titrations each) in total volumes of 55 mL using 30 μL or 50 μL steps with a minimum delay time between addition of standard base and pH measurement of 240 s. The establishment of equilibrium at each point of the titration curve was assured by preparing individual test solutions for some of the data points followed by pH measurement after an equilibration time of 2 days ("out of cell titration"). For determination of the protonation constants of **1**, 1:1 mixtures of Gd(III) and **3** ($c \approx 1.7$ mM) were titrated in the presence of a 1–2-fold molar excess of acid in a total volume of 30 mL.

The same procedures were used for determination of the acid dissociation constants of EDTA and DTPA and the stability constant of the Gd-DTPA complex for comparison and to indicate the validity of the equipment and methods used in this study.

Calculations of Equilibrium Constants. The calculations of all equilibrium stability constants were made with the computer program BEST.²⁵ This program iterates estimations of the equilibrium constants until an optimal fit of measured and calculated titration curves is reached. The absence of systematic deviations is an indication that all relevant species in the model were used for calculation. The differences between measured and calculated pH values (after optimization) in the relevant buffer regions were <0.01 units. For evaluation of the competition experiments with EDTA the literature value $\log K_{\text{GdL}} = 17.36$ ²⁶ and the protonation constants determined in this study were

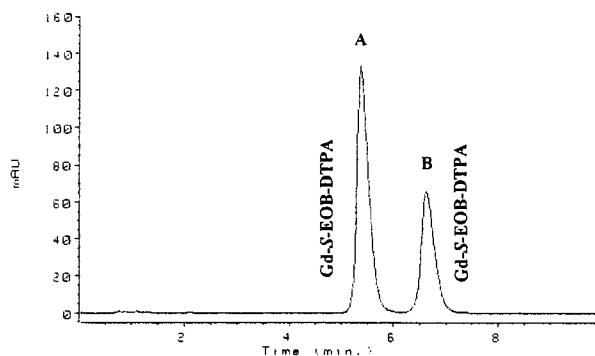


Figure 1. Separation of the diastereomers **A** and **B** of Gd-EOB-DTPA (**1**) with HPLC method 1.

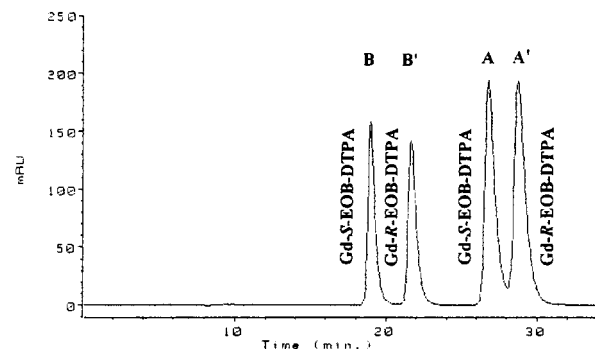


Figure 2. Separation of the pairs of diastereomers **A**, **B** and **A'**, **B'**, respectively, in a mixture of Gd-R-EOB-DTPA and Gd-S-EOB-DTPA (**1**) with HPLC method 2 (the order of elution of **A** and **B** is reversed compared to HPLC method 1).

used ($\log K_1 = 10.13$, $\log K_2 = 6.14$, $\log K_3 = 2.70$, $\log K_4 = 2.10$). The error of the results was estimated from the standard deviation of repeated determinations or from the propagation of an uncertainty of ± 0.02 units of the pH measurement.

HPLC Methods. The use of many different HPLC systems to separate the isomers of **1** resulted in the separation of two components with identical UV-spectra (ratio 65:35). Finally, HPLC method 1 (instrumentation: liquid chromatograph HP 1090 with diode array detector; column: 100×2.1 mm (i.d.) filled with ODS Hypersil 5 μm ; eluent: mixture of 460 g of 0.067 M phosphate buffer pH 7.5, 460 g of double distilled water and 63 g of acetonitrile at 25 °C; flow rate: 0.3 mL/min; detection: UV 225 nm) was used for quantification of the two components called isomers **A** and **B** according to the order of elution (Figure 1).

The chiral HPLC method 2 (instrumentation: liquid chromatograph HP 1090 with diode array detector; column: 250×4 mm (i.d.) filled with Chiradex 5 μm (Merck); eluent: mixture of 2 g of Na_2SO_4 in 30 mL of phosphate buffer pH 7.5, 110 mL of double distilled water and 60 mL of acetonitrile (Merck) at 25 °C; flow rate: 0.3 mL/min; detection: UV 225 nm) was able to separate both pairs **A**, **B** and **A'**, **B'** of the Gd complexes prepared from the enantiomeric ligands *S*-EOB-DTPA (**3**) and *R*-EOB-DTPA, the latter synthesized for comparison, which coelute under the conditions of HPLC method 1. The enantiomeric purity of the ligands *S*-EOB-DTPA (**3**) and *R*-EOB-DTPA determined by HPLC of their Gd -complexes with this method was $> 99.5\%$ (content of the other enantiomer $< 0.5\%$). The order of elution of the isomers **A**, **B** in this system is reversed in comparison to HPLC method 1 (Figure 2).

A preparative HPLC method 3 (instrumentation: HPLC pump series 3B, UV detector LC 75 Perkin-Elmer; column: 250×16 mm (i.d.) and precolumn 30×16 mm (i.d.) filled with ODS Hypersil 5 μm ; eluent: 2.5 g of NH_4HCO_3 in 940 mL of water (double distilled) and 60 mL of acetonitrile at room temperature; flow rate: 16 mL/min;

(24) Martell, A. E.; Smith, R. M. *Critical Stability Constants*; Plenum Press: New York, 1976; Vol. 4.

(25) Martell, A. E.; Motekaitis, R. J. *The Determination and Use of Stability Constants*, 2nd ed.; VCH: New York, 1992.

(26) Martell, A. E.; Smith, R. M. *Critical Stability Constants*; Plenum Press: New York, 1974 and 1982; Vols. 1 and 5.

injection: repeated injections of 12 mg portions of **1** in 400 μL of eluent; detection: UV 225 nm) was used for the isolation of sufficient amounts of the diastereomers **A** and **B** for the isomerization experiments.

Procedure for Isolation of the Isomers. A total amount of 135 mg of **1** was separated by repeated injections with HPLC method 3. The corresponding fractions were combined and concentrated at reduced pressure (ca. 0.5 h, 40 $^{\circ}\text{C}$, 40 mbar) in 0.5 L portions to remove the acetonitrile. For further enrichment, the remaining solutions (ca. 1 L solution of isomer **A** or 1.2 L solution of isomer **B**) were pumped separately on the preparative column with a HPLC pump after conditioning of the column with 2.5 g/L of NH_4HCO_3 solution. In this way, the isomers **A** or **B** were loaded on the column (no elution was observed under these conditions). Then the eluent was switched to 70% (v/v) methanolic NH_4HCO_3 solution, and the total amounts of the isomers **A** or **B** were collected in an eluate of ca. 20 mL. These eluates were evaporated (ca. 40 $^{\circ}\text{C}$, 40 mbar) to dryness. Under these conditions, NH_4HCO_3 was evaporated, too. Finally, 80 mg of isomer **A** and 44 mg of isomer **B** were obtained in solid form and stored in a refrigerator. To check the purity of the isolated products, small amounts were dissolved in Tris buffer pH 9 and analyzed with HPLC method 1.

Isomerization Experiments. Three samples of approximately 0.5 mg each of the isolated isomers were dissolved in 4 mL buffer solutions of pH 5, 6.8, and 9, respectively (pH 5: 0.07 M sodium acetate/HCl; pH 6.8: 0.1 M ammonium acetate, pH 9: 0.05 M Tris/HCl buffer; the measured pH value were pH 5, 7, and 9 at 25 $^{\circ}\text{C}$ and pH 5, 6.8 and 8.7 at 37 $^{\circ}\text{C}$). The test solutions were kept at 25 $^{\circ}\text{C} \pm 0.1$ $^{\circ}\text{C}$ or 37 $^{\circ}\text{C} \pm 0.1$ $^{\circ}\text{C}$. At appropriate time intervals (maximum time period ca. 3000 h for pH 9 at 25 $^{\circ}\text{C}$) samples were taken from the test solutions with a sterilized pipet and directly analyzed by HPLC (method 1) for the ratio of the isomers **A**:**B**. This procedure resulted in two series of measurements at each temperature and pH (first starting with **A** and the second starting with **B** to approach the equilibrium from both sides); see Figure 4. A further set of test solutions pH 5, pH 7, and pH 9 (pH at room temperature) was transferred to 100 μL glass vials and sealed with crimp caps directly before incubation at 120 $^{\circ}\text{C}$. Samples for analysis were taken after 0.5 h, 1.0, 2.0, and 3.0 h.

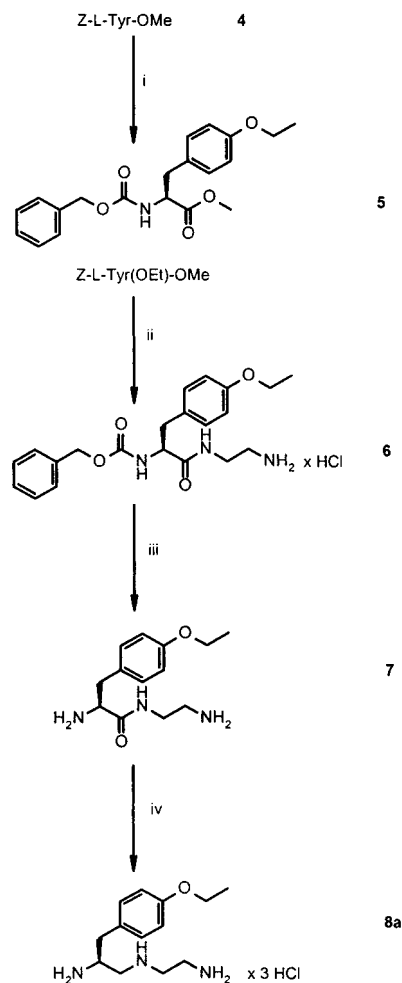
Results and Discussion

Our method for the synthesis of the gadolinium chelate **1** and the corresponding calcium complex **2** is shown in Schemes 1–3. Starting with the commercially available N_{α} -benzyloxycarbonyl-L-tyrosine methyl ester (*Z*-Tyr-OMe, **4**) we developed two different approaches to prepare the chiral triamine **8** as a key intermediate (Schemes 1 and 2). The triamine **8** was then converted in two steps into the nonstoichiometric sodium salt **13** that was used to prepare the gadolinium and the calcium chelates, respectively.

The details of this are that the protected amino acid *Z*-Tyr-OMe was *O*-alkylated at the phenolic function with ethyl iodide²⁷ in DMF, preferably using powdered potassium carbonate as base to yield *O*-ethyl- N_{α} -benzyloxycarbonyl-L-tyrosine methyl ester (**5**) in almost quantitative yield (98%). For the large-scale synthesis of **1**, two synthetic pathways leading to triamine **8** were investigated (Schemes 1 and 2).

The pathway shown in Scheme 1 corresponds to the synthesis of other C-substituted DTPA derivatives described in the literature:²⁸ Aminolysis of the amino acid methyl ester **5** with an excess of ethylenediamine followed by precipitation with HCl afforded *N*-(2-aminoethyl)- N_{α} -benzyloxycarbonyl-*O*-ethyl-L-tyrosinamide hydrochloride (**6**) with a yield of 69%. This was converted (86%) into *N*-(2-aminoethyl)-*O*-ethyl-L-tyrosinamide

Scheme 1. Synthesis of Triamine **8** via Diborane Reduction^a



^a Key: (i) $\text{C}_2\text{H}_5\text{I}$, K_2CO_3 , DMF, 20 h, rt; (ii) ethylenediamine (excess), methanol, 20 h, rt; (iii) H_2 , Pd/C, 15 atm, rt; toluene/aqueous KOH; (iv) diborane/THF, 80 $^{\circ}\text{C}$, 32 h; methanol; HCl (g).

(**7**) by catalytic hydrogenation.²⁹ For the subsequent reduction of the amide function with diborane/tetrahydrofuran the free diamine **7** was used instead of its hydrochloride salt due to the low solubility of the hydrochloride in tetrahydrofuran. To shorten the reaction time, the commercially available 1 M solution of diborane in tetrahydrofuran was concentrated as described in the Experimental Section. After acidic workup, the triamine *S*-1-(4-ethoxybenzyl)-3-azapentane-1,5-diamine was isolated (94%) as trihydrochloride **8a**.

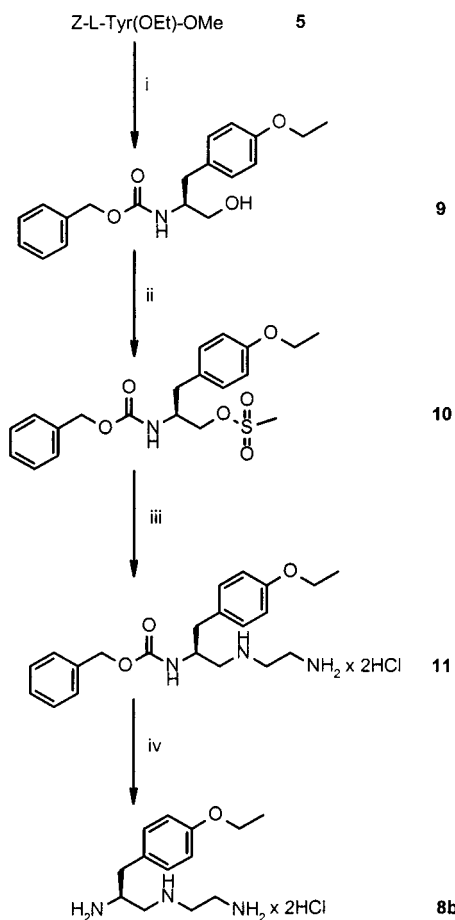
However, due to difficulties associated with the diborane/tetrahydrofuran procedure on a multikilogram scale, we developed the pathway shown in Scheme 2: Instead of aminolysis of tyrosine methyl ester **5**, the ester was reduced to the corresponding alcohol **9** using sodium borohydride in methanol.³⁰ After crystallization from hexane/ethyl acetate, **9** was isolated with a yield of 92%. Mesylation of (**9**) and further reaction with an excess of ethylenediamine and addition of aqueous HCl afforded the monoprotected triamine dihydrochloride **11** with a yield of 81%. Finally, catalytic hydrogenation afforded our key intermediate, the chiral triamine **8b** as the dihydrochloride (93%).

(27) Birosel, D. M. *J. Am. Chem. Soc.* **1931**, 53, 1408–1412.

(28) Brechbiel, M. W.; Gansow, O. A.; Atcher, R. W.; Schlom, J.; Esteban, J.; Simpson, D. E.; Colcher, D. *Inorg. Chem.* **1986**, 25, 2772–2781.

(29) Greene, T. W.; Wuts, P. G. M. *Protective Groups in Organic Synthesis*; John Wiley and Sons: New York 1991; p 335.

(30) Brown, M. S.; Rapoport, H. *J. Org. Chem.* **1963**, 28, 3261–3264.

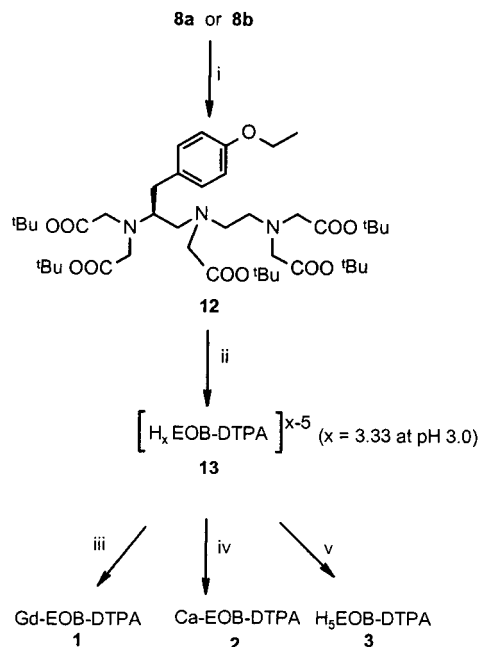
Scheme 2. Alternative Synthesis of Triamine **8** via Tyrosinol Derivative **9**^a

^a Key: (i) NaBH₄/THF; then methanol <30 °C; (ii) MesCl, Et₃N, THF, 0 °C; (iii) ethylenediamine (25 equiv); conc HCl; (iv) H₂, Pd/C, methanol, 1 h, 15 bar.

According to Scheme 3, both the trihydrochloride and the dihydrochloride, **8a** and **8b**, respectively, were treated with *tert*-butyl bromoacetate in tetrahydrofuran/water using potassium carbonate as base. The resulting crude product was subjected to preparative chromatography on reversed-phase silica gel yielding the oily penta-*tert*-butyl ester **12** with a yield of 73%. The most convenient deprotection method to generate the ligand EOB-DTPA was the use of sodium hydroxide in water/methanol rather than via the acidic standard procedures.³¹ We found that this smooth basic cleavage proceeds without any detectable side reactions. After cleavage of the *tert*-butyl groups the excess of sodium ions was removed by addition of cation-exchange resin Amberlite IR 120 (H⁺ form) to yield the sodium salt (94%) **13** with statistically 1.67 sodium ions per molecule at pH 3.0.

The complexation of **13** with Gd(III) was performed with gadolinium oxide in water at 80 °C to give the title compound **1** after neutralization with NaOH. Precipitation from water/ethanol (85%) yielded a material with a purity >98% as was shown by HPLC. Elemental analysis showed that the gadolinium complex isolated at pH 7.0 has 1.75 sodium ions per molecule.

The gadolinium complex of the enantiomeric ligand, Gd-*R*-EOB-DTPA, that was used in the HPLC study (see *infra*) was synthesized analogously starting with *D*-tyrosine instead of *L*-tyrosine.

Scheme 3. Synthesis of Gd-EOB-DTPA (**1**), Ca-EOB-DTPA (**2**), and the Free Ligand H₅EOB-DTPA (**3**)^a

^a Key: (i) BrCH₂COO^tBu, THF/H₂O, K₂CO₃, 20 h, reflux; chromatography; (ii) aqueous NaOH/methanol, 5 h reflux, overnight rt; IR 120 (H⁺) to pH 3; (iii) Gd₂O₃, 1 h, 80 °C, aqueous NaOH to pH 7; recrystallized from ethanol/H₂O; (iv) Ca(OH)₂, rt, 20 min, aqueous NaOH to pH 7; (v) IR 120 (H⁺) column, lyophilization.

Table 2. Bond Lengths in Å for **3**

N(1)–C(4)	1.505(5)	N(1)–C(8)	1.515(6)
N(1)–C(10)	1.518(5)	N(2)–C(9)	1.469(5)
N(2)–C(12)	1.468(6)	N(2)–C(16)	1.471(6)
N(3)–C(11)	1.511(5)	N(3)–C(20)	1.502(5)
N(3)–C(24)	1.509(6)	C(4)–C(5)	1.521(6)
C(5)–O(6)	1.311(5)	C(5)–O(7)	1.188(6)
C(8)–C(9)	1.524(6)	C(9)–C(34)	1.529(7)
C(10)–C(11)	1.520(6)	C(12)–C(13)	1.499(7)
C(13)–O(14)	1.199(6)	C(13)–O(15)	1.331(6)
C(16)–C(17)	1.500(6)	C(17)–O(18)	1.223(6)
C(17)–O(19)	1.307(6)	C(20)–C(21)	1.512(6)
C(21)–O(22)	1.208(6)	C(21)–O(23)	1.292(6)
C(24)–C(25)	1.503(6)	C(25)–O(26)	1.260(6)
C(25)–O(27)	1.228(6)	C(34)–C(49)	1.495(7)
C(49)–C(50)	1.376(7)	C(49)–C(54)	1.375(7)
C(50)–C(51)	1.376(7)	C(51)–C(52)	1.354(7)
C(52)–C(53)	1.376(7)	C(52)–O(55)	1.391(6)
C(53)–C(54)	1.366(7)	O(55)–C(56)	1.406(8)
C(56)–C(57)	1.459(8)		

Lanthanum-EOB-DTPA was synthesized as a structurally related diamagnetic complex for NMR characterization.

Calcium complex **2** used for the pharmaceutical formulation of **1** was prepared from the ligand **13** by reaction with calcium hydroxide.

The free ligand H₅EOB-DTPA **3** could be obtained on a preparative scale from **13** using an ion-exchange column and as crystalline material by slow evaporation of an aqueous solution of **3**.

The Ligand. The results of the X-ray analysis are summarized in Figure 3 and in Tables 1–3. Figure 3 shows the molecular conformation of **3** along with the atomic numbering scheme used in this X-ray study. All bond lengths and angles are in the range expected for this type of structure. The binding geometries of the carboxylate groups are indicative of noncharged moieties, especially because one hydrogen atom could be located for each of the carboxylic acid groups.

(31) Greene, T. W.; Wuts, P. G. M. *Protective Groups in Organic Synthesis*; John Wiley and Sons: New York, 1991; p 246.

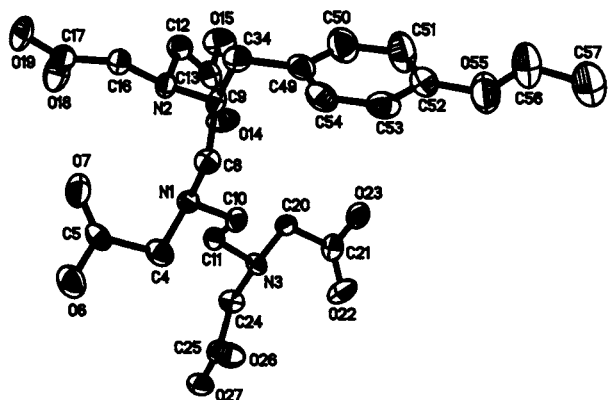


Figure 3. Molecular conformation and atomic numbering scheme for **3**. The anisotropic displacement coefficients are drawn at the 50% probability level; hydrogen atoms and water molecules have been omitted.

Table 3. Bond Angles (deg) for **3**

C(4)–N(1)–C(8)	109.0(3)	C(4)–N(1)–C(10)	110.2(3)
C(8)–N(1)–C(10)	111.3(3)	C(9)–N(2)–C(12)	111.5(3)
C(9)–N(2)–C(16)	112.4(3)	C(12)–N(2)–C(16)	111.1(3)
C(11)–N(3)–C(20)	111.6(3)	C(11)–N(3)–C(24)	108.1(3)
C(20)–N(3)–C(24)	111.8(3)	N(1)–C(4)–C(5)	109.4(3)
C(4)–C(5)–O(6)	110.5(4)	C(4)–C(5)–O(7)	123.1(4)
O(6)–C(5)–O(7)	126.4(4)	N(1)–C(8)–C(9)	111.6(3)
N(2)–C(9)–C(8)	109.3(3)	N(2)–C(9)–C(34)	116.5(4)
C(8)–C(9)–C(34)	109.5(4)	N(1)–C(10)–C(11)	108.6(3)
N(3)–C(11)–C(10)	109.8(3)	N(2)–C(12)–C(13)	112.5(4)
C(12)–C(13)–O(14)	124.9(4)	C(12)–C(13)–O(15)	111.1(4)
O(14)–C(13)–O(15)	124.0(4)	N(2)–C(16)–C(17)	115.7(4)
C(16)–C(17)–O(18)	124.6(4)	C(16)–C(17)–O(19)	111.2(4)
O(18)–C(17)–O(19)	124.1(4)	N(3)–C(20)–C(21)	112.2(4)
C(20)–C(21)–O(22)	120.9(4)	C(20)–C(21)–O(23)	113.3(4)
O(22)–C(21)–O(23)	125.8(4)	N(3)–C(24)–C(25)	111.2(4)
C(24)–C(25)–O(26)	115.0(4)	C(24)–C(25)–O(27)	118.3(4)
O(26)–C(25)–O(27)	126.7(4)	C(9)–C(34)–C(49)	113.9(4)
C(34)–C(49)–C(50)	120.5(4)	C(34)–C(49)–C(54)	122.9(4)
C(50)–C(49)–C(54)	116.5(4)	C(49)–C(50)–C(51)	122.4(5)
C(50)–C(51)–C(52)	119.8(5)	C(51)–C(52)–C(53)	119.1(5)
C(51)–C(52)–O(55)	126.0(5)	C(53)–C(52)–O(55)	115.0(4)
C(52)–C(53)–C(54)	120.6(5)	C(49)–C(54)–C(53)	121.6(4)
C(52)–O(55)–C(56)	117.7(4)	O(55)–C(56)–C(57)	109.3(5)

The presence of solvent water is often observed in the crystal structures of related compounds complexed with metal ions.^{32,33} Therefore, the presence of the additional maxima in the electron density distribution was expected. The assumption that these maxima correspond to water positions is supported by the following observations: (a) all water molecules have similar anisotropic displacement coefficients; (b) hydrogen atoms could be located for all of the water molecules; and (c) the distances between water oxygens and other oxygen atoms are in the range expected for hydrogen bonds.

The packing of **3** within the unit cell is stabilized by intermolecular hydrogen bonds involving all of the carboxylic acid groups and four water molecules. Most of the contacts between symmetry-related ligand molecules are mediated by water molecules, and only two direct interactions are observed (results are available in the Supporting Information).

The diffraction data were used to refine the parameter η for the determination of the absolute configuration. Although the errors are normally high in the absence of heavy atoms, this

parameter can be used to support results obtained with other methods. In this analysis, the value is refined to $\eta = 0.86(16)$. The theoretical value is 1.0, if the correct assignment of the configuration had been made (-1.0 if the original assignment was wrong). Therefore, the previously assumed $4S$ configuration of the compound could be confirmed experimentally.

The Gadolinium and Calcium Complexes. Protonation and Stability Constants. The results of the equilibrium studies with EOB-DTPA and DTPA, as obtained in this study under the same conditions and compared with literature data for DTPA (values in parentheses), are given in Table 4. The comparison of the protonation constants of both ligands indicates that the ethoxybenzyl side chain has almost no effect on the basicity of the ligand. The same is true for the complexation properties of the two ligands as is shown by the similarity of the stability constants of the respective Ca(II) and Gd(III) complexes. The slight increase of the stability constant of **1** compared to Gd-DTPA is accompanied by a slightly increased first protonation constant of **3** vs DTPA. This is in line with an analogous but less pronounced increase that is observed for BOPTA,²⁰ a DTPA derivative that is alkyl substituted at one of the terminal acetates. The conditional stability constant of **1** at physiological pH 7.4 is also given in Table 4. The complex stability of **2** is significantly smaller than that of **1**. This results in a considerably higher dissociation of **2** compared to **1** under the same conditions. Therefore, the addition of **2** to the pharmaceutical formulation of **1** acts as a ligand excess for minimizing the concentration of free Gd(III) and as a buffer for competing metal ions emerging during the shelf life of the drug product. On the other hand, the low stability constant of **2** indicates a high selectivity³⁴ of **3** for Gd(III) over Ca(II) by a factor of $10^{11.7}$, which is even somewhat higher than that of DTPA ($10^{10.7}$). Thus, no displacement of Gd(III) from **1** by Ca(II) can be expected under physiological conditions.

HPLC Separation and Kinetics of Equilibration of Diastereomeric Gadolinium Complexes. The ligand present in **1** is enantiomerically pure *S*-EOB-DTPA (**3**). Complex formation with Gd(III) generates a second chiral center, which gives rise to the existence of diastereomers. HPLC method 1 is able to separate two diastereomers called **A** and **B** in a ratio of approximately 65:35 (see Figure 1).³⁵ Both components coelute with the diastereomers **A'** and **B'** of the respective Gd-*R*-EOB-DTPA, which was synthesized for comparison. However, the chiral HPLC method 2 separates both pairs, **A**, **B** from Gd-*S*-EOB-DTPA (**1**) and **A'**, **B'** from Gd-*R*-EOB-DTPA (see Figure 2).

To follow the isomerization of **A** and **B** as dependent on pH and temperature sufficient amounts of both diastereomers were isolated by HPLC method 3. Figure 4 shows an example for the two sets of results, which were obtained in the isomerization experiments at each pH and temperature by starting either with pure isomer **A** or with pure isomer **B**.

The data indicate an equilibrium of the type



(32) Aime, S.; Barge, A.; Benetello, F.; Bombieri, G.; Botta, M.; Uggeri, F. *Inorg. Chem.* **1997**, *36*, 4287–4289.

(33) Porai-Koshits, M. A.; Shkol'nikova, L. M.; Sadikov, G. G.; Davidovich, R. L.; Fundamenskii, V. S.; Shchurkina, V. N.; Valyaeva, M. E. *Russ. J. Inorg. Chem.* **1994**, *39*, 1724–1733.

(34) Cacheris, W. P.; Quay, S. C.; Rocklage, S. M. *Mag. Reson. Imag.* **1990**, *8*, 467–481.

(35) The same method is also able to separate two diastereomers of the analogous La-EOB-DTPA complex in a 60:40 ratio.

Table 4. Complex Stability Constants of EOB-DTPA and DTPA Complexes and Protonation Constants of the Ligands (at 25 °C in 0.1 M KCl) (Values in Parentheses Are Literature Values for Comparison²⁶)

equilibrium	log K	
	L = EOB-DTPA	L = DTPA
$K_{HL} = [HL^{4-}]/[L^{5-}][H^+]$	10.91 ± 0.04	10.34 ± 0.05 (10.49)
$K_{H2L} = [H2L^{3-}]/[HL^{4-}][H^+]$	8.63 ± 0.01	8.59 ± 0.02 (8.60)
$K_{H3L} = [H3L^{2-}]/[H2L^{3-}][H^+]$	4.26 ± 0.01	4.25 ± 0.03 (4.28)
$K_{H4L} = [H4L^-]/[H3L^{2-}][H^+]$	2.73 ± 0.02	2.71 ± 0.07 (2.64)
$K_{H5L} = [H5L]/[H4L^-][H^+]$	2.08 ± 0.06	2.18 ± 0.25 (2.0)
$K_{CaL} = [CaL^{3-}]/[Ca^{2+}][L^{5-}]$	11.74 ± 0.02	11.77 ± 0.08 (10.75)
$K_{CaLH} = [CaLH^{2-}]/[CaL^{3-}][H^+]$	5.75 ± 0.03	6.10 ± 0.01 (6.11)
$K_{CaLH2} = [CaLH2^-]/[CaLH^{2-}][H^+]$	4.16 ± 0.1	
$K_{Ca2L} = [Ca2L^-]/[CaL^{3-}][Ca^{2+}]$	2.18 ± 0.2	
$K_{GdL} = [GdL^{2-}]/[Gd^{3+}][L^{5-}]$	23.46 ± 0.13	22.52 ± 0.3 (22.46)
	18.7 ^a	18.4 ^a
$K_{GdLH} = [GdHL^-]/[GdL^{2-}][H^+]$	2.17 ± 0.08	(2.39)

^a Conditional stability constant at $-\log [H^+] = 7.4$.

Table 5. Mean Values of Kinetic and Equilibrium Data of Isomerizations **A** → **B** and **B** → **A** as a Function of Temperature and pH

T (°C)	pH	k_1 (h ⁻¹)	$t_{1/2}$ (h)	$A_{\infty}:B_{\infty}$
25	5.0	2.97×10^{-1}	2.34	64.8:35.2
	7.0	4.59×10^{-3}	150.9	64.6:35.4
	9.0	5.28×10^{-5} ^b	13100 ^b	d
37	5.0	6.86×10^{-1}	1.01	65.3:34.7
	6.8	1.56×10^{-2}	44.5	64.8:35.2
	8.7	1.94×10^{-4}	3592	d
120	5.0 ^a	>4.1	<0.17	65.2:34.8
	6.8 ^a	>4.1	<0.17	63.5:36.5
	9.0 ^a	1.83 ^c	0.39 ^c	64.1:35.9

^a Measured at 25 °C. ^b Only from isomerization **B** → **A** due to low conversion of isomerization **A** → **B** at the end of the experiment (~3000 h). ^c Rough estimation due to lack of data points. ^d Estimates are uncertain due to low conversion at the end of the experiment.

which can be described by the following rate laws

(1) start with pure **A**

$$\ln \frac{A - A_{\infty}}{A_0 - A_{\infty}} = -(k_{AB} + k_{BA})t \quad (3)$$

$$= -k_1 t$$

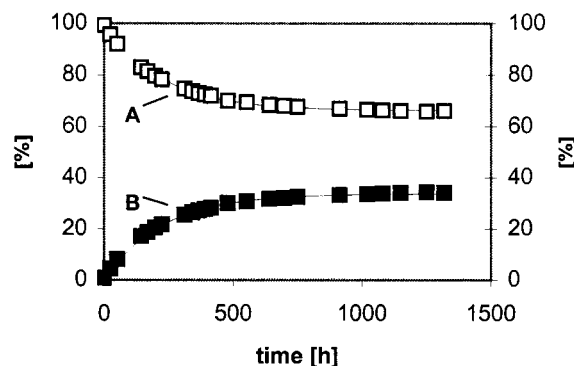
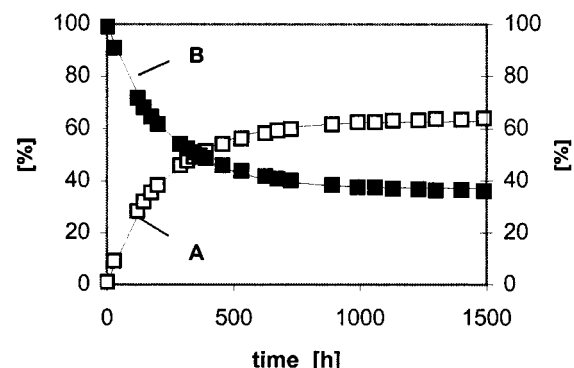
(2) start with pure **B**

$$\ln \frac{B - B_{\infty}}{B_0 - B_{\infty}} = -(k_{AB} + k_{BA})t \quad (4)$$

$$= -k_1 t$$

where A , B are the concentration of **A**, **B** at time t in % of initial; A_0 , B_0 are the concentrations of **A**, **B** at time $t = 0$ (100%); A_{∞} , B_{∞} are the concentrations of **A**, **B** at equilibrium in %; k_{AB} is the first-order rate constant of the reaction **A** → **B** in h⁻¹; k_{BA} is the first-order rate constant of the reaction **B** → **A** in h⁻¹; k_1 is the first-order rate constant of the equilibration **A** → **B**, when starting with pure **A** or **B** ($k_1 = k_{AB} + k_{BA}$) in h⁻¹, the corresponding half-life of equilibration, i.e., time for reaching $(A_0 - A_{\infty})/2$ or $(B_0 - B_{\infty})/2$, is $t_{1/2} = \ln 2/k_1$; and t is the time in h.

The two series of data after starting with pure **A** or pure **B** at each pH value and temperature were evaluated with the computer program TopFit 2.0³⁶ to give estimates for k_{AB} , k_{BA} , A , and B according to the model shown above. The mean results of each of the two series ($k_1 = k_{AB} + k_{BA}$, $t_{1/2}$ = half-life of

Gd-EOB-DTPA Isomerization A → B
(25 °C, pH 7)**Gd-EOB-DTPA Isomerization B → A**
(25 °C, pH 7)**Figure 4.** Example for the equilibration of both isomers **A** and **B** of **1** at pH 7, 25 °C

equilibration and $A_{\infty}:B_{\infty}$ = estimated ratio **A**:**B** at equilibrium) are summarized in Table 5.³⁷

The ratio of the isomers in equilibrium **A**:**B** = 65:35 is independent of temperature and pH (range $T = 25$ – 120 °C, pH 5–9) within the experimental error as to be expected for an equilibrium near 1:1. The pH dependence of the rate constant

(36) Heinzel, G.; Woloszczak, R.; Thomann, P. *Pharmacokinetic and Pharmacodynamic Data Analysis System for the PC*; Gustav Fischer Verlag: Stuttgart, 1993.

(37) Preliminary experiments with the isomers of La-EOB-DTPA indicated equilibration times of < 0.5 h at pH 5, approximately 20 h at pH 7, and > 200 h at pH 9 (all at room temperature), which are significantly shorter than those of **1**.

k_1 for equilibration of the diastereomers **A** and **B** of **1** suggests that the isomerization is an acid-catalyzed process similar to the dissociation of **1** (kinetic data are also available³⁸). Therefore, a pseudo-first-order rate constant of isomerization can be postulated according to

$$k_1 = k_2 \cdot [\text{H}^+] \quad (5)$$

or

$$\log k_1 = \log k_2 - \text{pH} \quad (6)$$

k_2 is the second-order rate constant for equilibration of these diastereomers, which is independent of the hydrogen ion concentration $[\text{H}^+]$. The linear regression calculations of $\log k_1$ versus pH according to eq 6 give a slope of -0.93 and intercept of 4.14 for the data at 25°C and a slope of -0.96 and intercept of 4.66 for the data at 37°C . The slopes of the regression lines, obtained with three data points at each temperature, are in reasonable agreement with the postulated value of -1 for a proton-catalyzed process.

The intercepts of the regression lines correspond to second-order rate constants $k_2 = 1.41 \times 10^4 \text{ h}^{-1} \text{ M}^{-1}$ at 25°C and $k_2 = 4.57 \times 10^4 \text{ h}^{-1} \text{ M}^{-1}$ at 37°C . By applying the Arrhenius relation to these data, the activation energy for the equilibration of the diastereomers of **1** can be approximated by

$$E_A = 75.3 \text{ kJ mol}^{-1}$$

This value is a rough estimate since it is derived from two data points only, which are relatively close to each other. Therefore, no extrapolation over a greater temperature range should be made on the basis of this value. Nevertheless, the extrapolation to 120°C and pH 9 (with consideration of a buffer pH shift of -0.028 pH unit/K) gives a value for the rate constant for the equilibration of the isomers, which is in the order of magnitude of the experimental values given in Table 5.

The Structure of the Diastereomers of 1. So far, all attempts to crystallize **1** and to determine its structure by X-ray crystallography have failed. However, the solution structure of the analogous diamagnetic complex anion $[\text{La-S-EOB-DTPA}]^{2-}$ can be determined by NMR. ^1H and ^{13}C NMR spectra revealed a 60:40 ratio of two isomers. This corresponds to the HPLC separation of La-EOB-DTPA that showed also the presence of two isomers in a 60:40 ratio.^{35,36} Therefore, the structures of the diastereomers of **1** should be derived with confidence from the corresponding lanthanum structures. However, it is important to note that the deduction of the structures of **1** from the lanthanum complex should be done with care due to the relatively small differences in the relative energies between the diastereomers of each complex and the well-known differences of the ionic radii of La(III) and Gd(III).

Theoretically, structures of four possible diastereomers of the complex anion $[\text{Gd-S-EOB-DTPA}]^{2-}$ can be derived in a systematic manner starting from the experimentally determined X-ray structure of $[\text{Gd-DTPA}]^{2-}$.³⁹ In the crystalline state, the complex anion $[\text{Gd-DTPA}]^{2-}$ is present in two different forms that are mirror images of each other. The Gd(III) ion is 9-fold coordinated. Eight coordination sites are occupied by atoms of the ligand DTPA, and the ninth coordination site is occupied by the oxygen atom of a water molecule. The orientation of the acetate groups of the ligand DTPA is best depicted as the

orientation of a propeller blade, i.e., right- or left-handed, or described in a formal way using stereochemical descriptors as $[\text{SA-8-11131423-C}]$ and $[\text{SA-8-11131423-A}]$.^{40,41}

The introduction of the ethoxybenzyl group into the 4-position of the 3,6,9-triazaundecandioate system differentiates between the 4- and the 8-positions which are equivalent in the unsubstituted Gd-DTPA complex. The central nitrogen atom becomes chiral upon complexation, and the configuration of the two diastereomers thus generated can be described as (4*S*,6*S*) and (4*S*,6*R*), respectively. Taking into account the two possible orientations of the acetate groups, a total of four diastereomers $[\text{SA-8-11252634-A-S}]\text{-1}$, $[\text{SA-8-12253614-A-S}]\text{-1}$, $[\text{SA-8-12253614-C-S}]\text{-1}$, and $[\text{SA-8-11252634-C-S}]\text{-1}$ are generated for the complex anion $[\text{Gd-EOB-DTPA}]^{2-}$. The corresponding structures are shown as schematic drawings in Figure 5a (4*S*,6*S*) and Figure 5b (4*S*,6*R*).⁴² Conformers which will result from different dihedral angles of the ethylene bridges are not discussed.

For the closely related Ln-DOTA complexes, diastereomers that result from different orientations of the acetate groups or from different dihedral angles of the ethylene bridges of the tetraazacyclododecane ring are not separable by HPLC techniques. Nevertheless, such diastereomers have been characterized by ^1H and ^{13}C NMR spectroscopy.^{43,44} In the solid state, the presence of two forms that differ only in the orientation of the acetate groups for Ln = Eu,⁴⁵ Gd,^{46,47} and Lu⁴⁸ and for Ln = La³² was shown by X-ray crystallography.

An assignment of the diastereomers **A** and **B** has to take into account the available interpretation of NMR data of the structurally related diamagnetic complex anion $[\text{La-S-EOB-DTPA}]^{2-}$. By detailed NMR experiments at elevated temperature the major component (60%) observed was assigned to the (4*S*,6*R*) and the minor isomer (40%) to the (4*S*,6*S*) diastereomer, respectively.^{49,50} Therefore, it is concluded that the diastereomers **A** and **B** observed in the HPLC separation of **1** differ in the chirality of the central nitrogen or, in other words, in the orientation of the ethoxybenzyl substituent (Figure 5a,b). However, both isolated components **A** and **B** are probably mixtures of diastereomers that differ in the orientation of the acetate groups: the pair of diastereomers $[\text{SA-8-11252634-A-S}]\text{-1}$ and $[\text{SA-8-12253614-A-S}]\text{-1}$ and the pair of diastereomers $[\text{SA-8-11252634-C-S}]\text{-1}$ and $[\text{SA-8-11252634-C-S}]\text{-1}$, respectively. The NMR studies of the diamagnetic complex anion $[\text{La-S-EOB-DTPA}]^{2-}$ gave no evidence for the presence of diastereomers that differ in the orientation of the acetate groups, most probably due to the fast interconversion of these isomers on

(38) Brücher, E. et al. Manuscript in preparation.

(39) Gries, H.; Miklautz, H. *Physiol. Chem. Phys. Med. NMR* **1984**, *16*, 105–112.

(40) Brown, M. F.; Cook, B. R.; Sloan, T. *Inorg. Chem.* **1978**, *17*, 1563–1568.

(41) The chirality symbols *C* (clockwise) and *A* (anticlockwise) are not related to the orientation of the propeller blade.

(42) Seen from the water oxygen at the ninth position on top of the square antiprism.

(43) Aime, S.; Botta, M.; Ermondi, G. *Inorg. Chem.* **1992**, *31*, 4291–4299.

(44) Hoefst, S.; Roth, K. *Chem. Ber.* **1993**, *126*, 869–873.

(45) Spirlet, M. R.; Rebizant, J.; Desreux, J. F.; Loncin, M. F. *Inorg. Chem.* **1984**, *23*, 359–363.

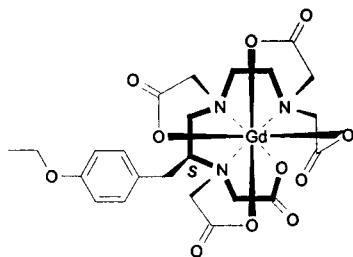
(46) Dubost, J. P.; Legar, J. M.; Langlois, M. H.; Meyer, D.; Schaefer, M. C. R. *Acad. Sci., Paris Ser. II* **1991**, *312*, 349–354.

(47) Chang, C. A.; Francesconi, L. C.; Malley, M. F.; Kumar, K.; Gougoutas, J. Z.; Tweedle, M. F.; Lee, D. W.; Wilson, L. J. *Inorg. Chem.* **1993**, *32*, 3501–3508.

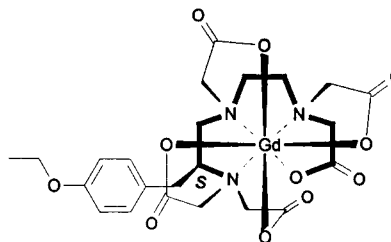
(48) Aime, S.; Barge, A.; Botta, M.; Fasano, M.; Ayala, J. D.; Bombieri, G. *Inorg. Chim. Acta* **1996**, *246*, 423–429.

(49) Hoefst, S. Über die Struktur und Dynamik von Lanthanoid-Chelatkomplexen. Ph.D. Thesis, FU Berlin, D81, 1995

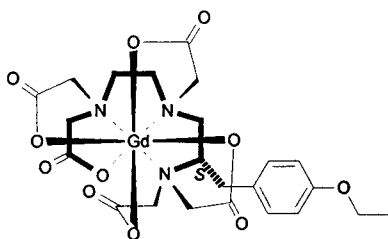
(50) Hoefst, S.; Bermel, W.; Radüchel, B.; Schmitt-Willich, H.; Roth, K. Proceedings of the Society of Magnetic Resonance, 2nd meeting, August 6–12, 1994, San Francisco, CA.

a) (*4S,6S*) diastereomers:

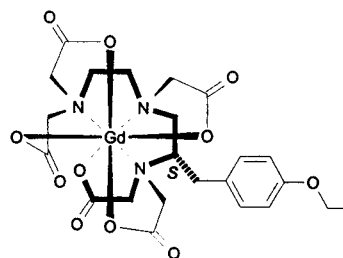
[SA-8-11252634-A-S] ("left handed propeller blade")



[SA-8-12253614-A-S] ("right handed propeller blade")

b) (*4S,6R*) diastereomers:

[SA-8-12253614-C-S] ("left handed propeller blade")



[SA-8-11252634-C-S] ("right handed propeller blade")

Figure 5. Structures of the four diastereomers of **1**.

the NMR time scale.^{32,45} A definitive assignment is only possible on the basis of theoretical calculations of the relative energies of the different diastereomers for the dia- and paramagnetic complexes.

The interpretation of our HPLC results is in line with a corresponding HPLC study of the complex anions [Y-4-(4-aminobenzyl)-DTPA]²⁻ and [Y-4-(4-aminobenzyl)-8-methyl-DTPA]²⁻, which were separated into two and three components, respectively.⁵¹

Conclusions

Two different synthetic approaches have been developed to prepare the chiral triamine **8**, which is the key intermediate in the synthesis of Gd-EOB-DTPA, **1**. Thus, large-scale production of this novel liver-specific MRI contrast agent has become available by replacing the commonly used diborane procedure with a new alkylating protocol in one of the described synthetic pathways leading to **8**.

The data presented on the stability and protonation constants of **1–3** indicate the similarity of the ethoxy-substituted EOB-DTPA to the unsubstituted DTPA. However, the first protonation constant of **3** is slightly larger than that observed for DTPA

under similar conditions. This increase is likely to be the origin of the enhanced stability constant for **1** vs Gd-DTPA.

Chelation of the chiral ligand **3** with Gd(III) should give rise to four diastereomers, at least in the solid state. So far, all attempts to crystallize **1** and to determine its structure by X-ray crystallography have failed. However, two diastereomeric gadolinium complexes present in aqueous solution of **1** have been isolated. The investigation of the kinetics of isomerization of these two complexes as dependent on the temperature allowed an estimate of 75.3 kJ mol⁻¹ for the activation energy for the interconversion of **A** and **B**. Structures for the two diastereomers are proposed on the basis of available NMR data of the analogous La-EOB-DTPA complex. It is concluded that the isolated components **A** and **B** differ in the chirality of the central nitrogen and that both **A** and **B** are mixtures of diastereomers with different orientations of the acetate groups.

Acknowledgment. The excellent technical assistance of Mr. W. Behrendt and Mr. K. Weigandt is gratefully acknowledged. We also thank Dr. A. Cleve for his help with the nomenclature of the complexes.

Supporting Information Available: Tables of crystallographic data, atomic parameters, complete bond lengths and bond angles, and anisotropic thermal parameters. This material is available free of charge via the Internet at <http://pubs.acs.org>.

(51) Cummins, C. H.; Rutter, E. W.; Fordyce, W. A. *Bioconjugate Chem.* **1991**, *2*, 180–186.